SIMPLIFIED METHODOLOGY TO ESTIMATE EARTHQUAKE-INDUCED EXPECTED LIFE CYCLE COSTS OF LOW-RISE STEEL BUILDINGS

G. Araya-Letelier[1], L. Eads[2]

[1] *Assistant Professor, Faculty of Engineering and Sciences, Universidad Adolfo Ibáñez, Santiago, Chile, gerardo.araya@uai.cl*
[2] *Senior Modeler, Risk Management Solutions, London, UK, laura.eads@rms.com*

Abstract

Seismic design codes are primarily aimed at protecting human life, but they are not intended to minimize or even calculate the earthquake-induced economic losses that a building might experience during its service life. Fortunately, the Performance Based Earthquake Engineering (PBEE) framework introduced by the Pacific Earthquake Engineering Research (PEER) Center allows evaluation of decision variables such as earthquake-induced economic losses, downtime, fatalities and environmental impacts. The evaluation of these decision variables shows the level of performance of a given structure, allowing owners and stakeholders the selection of higher levels of performance if they are not satisfied with the minimum code requirements. These higher levels of performance are associated with higher initial investments that also need to be estimated to provide complete information for a satisfactory decision-making process. However, the computation of economic losses under the PEER-PBEE framework is very time consuming to conduct on a routine basis.

These difficulties highlight the importance of simplified methodologies to calculate building-specific earthquake-induced economic losses towards optimizing the structural design, and significant work has been developed in this area since the early 1970s. However, these simplified methods are still not widely used in real practice. Therefore, more research is needed towards developing simpler methodologies (based on the PEER-PBEE framework) that can be used in performance-based design. Consequently, this study develops a simplified methodology to estimate the earthquake-induced expected life cycle cost (ELCC) of buildings, which is the summation of the expected construction cost (CC) and the net present value of the earthquake-induced expected annual loss (EAL). In particular this study focuses on low-rise steel special moment-resisting frame (SMRF) buildings since these structures are very flexible, first-mode dominated, and their EAL values are dominated by small spectral acceleration (S_a) intensities where the structures are behaving linearly or under the equal displacement rule, presenting a distribution of engineering demand parameters, such as peak story drift ratios (PSDR), that is relatively uniform along the height of the structure.

To develop the simplified methodology, firstly a series of 4-story steel SMRF buildings are designed with varying degrees of lateral stiffness. While designs are code-conforming, the variation in lateral stiffness affects the ELCC of the structure. The ELCC of each structure is assessed via the PEER-PBEE framework, using nonlinear response history analyses in OpenSees to perform seismic simulations and commercially available construction cost databases to estimate variations in construction costs. Based on these numeric results, this simplified methodology is developed and calibrated to estimate the ELCC as a function of the fundamental period of vibration (T_1) for low-rise SMRF buildings. For the estimation of the CC, this study extends previous work, and for the estimation of the EAL this study develops a closed-form solution that does not require performing incremental dynamic analyses and numerical integrations. Finally, approximate values obtained using the proposed simplified methodology are compared to exact numeric values obtained using the PEER-PBEE framework for a series of 4-story steel SMRF buildings designed, and results are promising.

Keywords: simplified methodology, loss estimation, earthquake-induced expected life cycle cost, steel buildings

1. Introduction

Seismic design codes are primarily aimed at protecting human life, which has been successfully demonstrated in recent large earthquakes in Chile and New Zealand [1, 2] where the number of fatalities due to collapsed buildings was relatively low. However, the economic losses experienced in these countries were significant, pointing out that owners and stakeholders may desire performance objectives that go beyond the minimum code requirements to reduce these earthquake-induced economic losses. To face these challenges, the fully probabilistic PBEE framework introduced by PEER allows assessing decision variables such as earthquake-induced economic losses, downtime, fatalities [3] and environmental impacts. The quantitative evaluation of these decision variables shows the level of performance of a given structure, allowing owners and stakeholders to select higher levels of performance if they are not satisfied with the minimum code requirements. These higher levels of performance are associated with higher initial investments that also need to be estimated to provide complete information for a satisfactory decision-making process. However, the computation of economic losses under the PEER-PBEE framework requires large data sets, estimating the response of the structure under study and several integrations of many random variables, among other things. These requirements can make the implementation of this framework very time consuming, making it prohibitively expensive to conduct on a routine basis [4]. The framework also requires engineers well trained in topics such as probability theory and nonlinear dynamic analyses.

These difficulties highlight the importance of simplified methodologies to calculate building-specific earthquake-induced economic losses towards optimizing the structural design, and significant work has been developed in this area since the early 1970s. Vanmarcke et al. [5] introduced a Markov decision theory methodology for optimum seismic design, accounting in a simplified way for the trade-off between higher construction costs in seismic structural designs and reduction in future earthquake-induced economic losses. This might be the first formal approach towards an optimum seismic design minimizing the ELCC of structures, which is the summation of the CC and the net present value (NPV) of the EAL over a period of time. Other researchers [6-8] also worked on optimum seismic design but focused on minimizing the CC that satisfied a particular seismic performance constraint. More recent studies have investigated simplified methodologies to calculate earthquake-induced economic losses and to implement performance-based seismic design minimizing these losses [9-11]. Additionally, the Applied Technology Council (ATC) through the ATC-58 project [12] released performance-based seismic design procedures trying to expose the practicing-engineering community to these new advances in loss estimation and performance-based design. However, these simplified methods are still not widely used in practice. Therefore, more research is needed towards developing simpler methodologies based on the PEER-PBEE framework that can be used in performance-based design. Consequently, this study develops a simplified methodology to estimate the ELCC of buildings. In particular this study focuses on low-rise steel SMRF buildings since these structures are very flexible, first-mode dominated, and their EAL values are dominated by small S_a intensities where the structures are behaving linearly or under the equal displacement rule, resulting in a distribution of engineering demand parameters, such as PSDR, that is relatively uniform along the height of the structure. For the estimation of the CC, this study extends previous work by Reyes [13], and for the estimation of EAL, this study develops a closed-form solution based on previous work [14-16]. The proposed methodology can be used to analyze the variation of the ELCC as a function of the stiffness, expressed in terms of T_1, of a low-rise steel SMRF building and, therefore, to find the value of T_1 that minimizes the ELCC.

2. Earthquake-Induced Expected Life Cycle Cost

The ELCC analysis is defined as an economic assessment of an item, system or facility that considers all the significant expected costs of ownership over its economic life, in terms of equivalent dollars [17]. Focusing on seismic damage, the ELCC of a building is shown in Eq. (1).

$$ELCC = CC + NPV(EAL) \tag{1}$$

where ELCC and CC have been defined, NPV(EAL) is the net present value of the EAL of the building as a result of earthquake damage during its service life, and the EAL represents the average economic loss that is obtained every year from seismic damage to the building.

For a specific building the CC can be estimated from available construction cost data publications, such as RSMeans [18], that allow the estimation of the CC for buildings with different structural configurations, structural materials, geometries, uses, locations, etc. These costs are representative of standard buildings, which are code-conforming designs that usually only meet the minimum code requirements.

The NPV(EAL) term is the financial function NPV() that brings to present time the future EAL for each year considering the service life of the building and including a real discount rate, as shown in Eq. (2).

$$NPV(EAL) = \sum_{i=1}^{m} \frac{EAL}{(1+RDR)^i} \tag{2}$$

where RDR is the annual real discount rate (that considers the effect of future inflation/deflation), m is the number of years considered for the service life of the building, and the EAL is calculated as shown in Eq. (3).

$$EAL = \int_{S_a=0}^{\infty} E[L|S_a] \left| \frac{d\lambda(S_a)}{dS_a} \right| dS_a \tag{3}$$

where $E[L|S_a]$ is the expected economic loss conditioned on S_a and $\left| \frac{d\lambda(S_a)}{dS_a} \right|$ is the absolute value of the derivative of the seismic hazard curve considering S_a for a specific value of T_1, damping, and site.

For alternative levels of performance of a given lateral force-resisting system, the trade-off between enhanced seismic performance, which reduces the NPV(EAL), and higher CC can be evaluated through the computation of the ELCC for each alternative, providing an effective metric to support the decision-making process towards the selection of a desired performance level. For instance, the minimum ELCC would be the optimum design for a risk neutral decision maker, whose decisions are based on expected values.

3. ELCC Assessment: Full Methodology Implementation

To develop this simplified methodology, six additional SMRF designs of a code-conforming testbed 4-story steel SMRF building are developed with varying degrees of lateral stiffness. While designs are code-conforming, the variation in lateral stiffness affects the ELCC of the structure. The EAL and CC of each structure are obtained using the PEER-PBEE framework and the RSMeans construction database [18], respectively.

3.1 Testbed building, alternative SMRF designs and construction costs

The testbed building used in this study is a four-story code-conforming steel prototype office building designed by Lignos and Krawinkler [19] for vertical and lateral loads. The structural system is an A992 Grade 50 steel SMRF with fully restrained reduced beam sections. Dimensions are 36.4 m by 27.3 m in plan (see Fig.1(a)). The first story is 4.6 m tall, and the rest of the stories are 3.7 m tall (see Fig.1(b)). Values of T_1 are 1.33 s and 1.22 s for the east-west (EW) and north-south (NS) directions, respectively. The seismic performance of the building is evaluated using a two-dimensional model of the SMRF in the EW direction, which is highlighted in Fig.1(a) and shown in elevation in Fig.1(b).
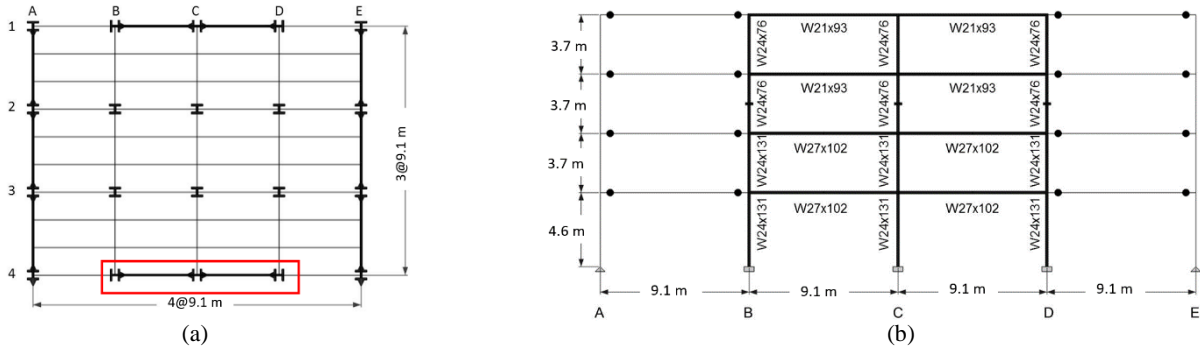

Fig. 1 –Testbed building geometry: a) plan highlighting EW SMRF; b) elevation of EW SMRF evaluated

Although the performance simulations of this study are limited to EW frames, alternative SMRF designs are developed in both directions to perform cost-benefit analyses since frames in the NS direction should have a stiffness consistent with the EW direction. Thus, the CC for each alternative design incorporates the variation in steel and foundation costs for the EW as well as NS frames. The alternative SMRF designs are based on the PSDR desired for the design basis earthquake (DBE). Miranda [20] proposed Eq. (4) to estimate the elastic PSDR.

$$PSDR = \beta_1 \beta_2 \frac{S_d}{H_{roof}} \qquad (4)$$

where β_1 is a shape factor that depends on the lateral resisting system, the height of the building and the load distribution, β_2 is a concentration factor that converts average story drift ratio to the PSDR that the building undergoes at any story, S_d is the elastic spectral displacement corresponding to T_1 of the building, and H_{roof} is the height of the building. Eq. (4) is based on a multi-degree-of-freedom system application of the equal displacement rule, which is a reasonable assumption for a low-rise steel SMRF building. Using Eq. (4) and the design response spectrum for the selected site (33.996, -118.162, and class D) obtained from the United States Geological Survey (USGS) [21] the PSDRs for the DBE at different values of T_1 are estimated as shown in Table 1. These seven levels of PSDR are associated with particular target values of T_1 that were used to develop specific SMRF designs (except for the testbed building that was already designed). The actual values of T_1 as well as the CCs (normalized by the CC of the testbed building) for each SMRF design are also in Table 1. Note that the most flexible design (T_1=1.86 s) has a PSDR larger than 3% at the DBE, which does not meet code requirements and was designed only for research purposes. For further information see Araya-Letelier [22].

Table 1 – Design response spectrum for selected site (33.996, -118.162, and class D), corresponding estimation of PSDR as a function of target values of T_1 and actual values of T_1 and CC for each SMRF design

#	Target T_1 [s]	S_a [g]	S_d [cm]	PSDR [%]	Actual T_1 [s]	CC (US$)	CC (%)
1	0.52	1.16	7.90	0.9%	0.49	8,234,448	109.8%
2	0.60	1.01	9.07	1.1%	0.63	7,936,015	105.8%
3	0.70	0.87	10.57	1.2%	0.73	7,783,672	103.7%
4	0.80	0.76	12.07	1.4%	0.82	7,682,648	102.4%
5	1.00	0.61	15.09	1.8%	1.04	7,579,729	101.0%
6	1.30	0.47	19.63	2.3%	1.33	7,502,976	100.0%
7	1.80	0.34	27.18	3.2%	1.86	7,385,144	98.4%

3.2 Site and seismic hazard curves

The testbed building is located in southern California (33.996, -118.162). This site is classified as class D and has been analyzed by previous researchers [22, 23] because it is a typical urban site in California with high seismicity, located within 20 km of seven faults, but not subjected to near fault directivity effects [23]. The design spectrum for the DBE at the site, shown in Fig.2, and the seismic hazard curves ($\lambda(S_a(T_1,5\%))$), shown in Fig.3, were obtained using data from the USGS [21]. Linear interpolation in the log-log domain was used to obtain the seismic hazard curves for values of T_1 not listed by the USGS. This interpolation is assumed to be adequate since the T_1 values of the SMRFs are mostly located within the descending branch of the design spectrum where the variation of S_a is inversely proportional to T_1. Additionally, 7th-order polynomials are fitted in the log-log domain to represent the seismic hazard curves as continuous functions for later numerical integrations.
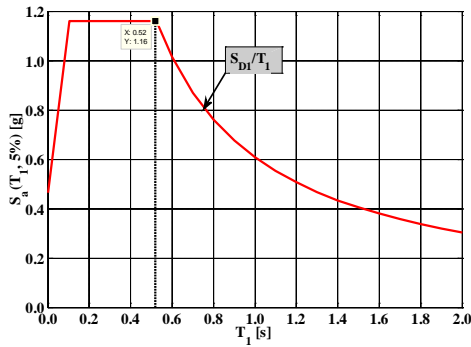
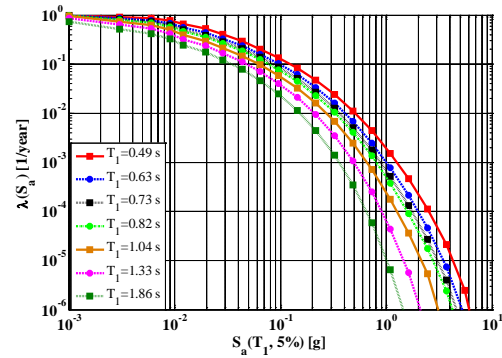Fig. 2 –Design spectrum for selected site

Fig. 3 – Seismic hazard curves for SMRF designs

3.3 Seismic response simulations

The seven SMRF designs were subjected to incremental dynamic analyses (IDAs) using the OpenSees platform. These IDAs consisted of a set of 80 ground motions with S_a increments of 0.1 g, from zero all the way to collapse for each ground motion. Engineering demand parameters (EDPs) of interest for each SMRF design are PSDRs, residual story drift ratios (RSDRs) and peak floor accelerations (PFAs) for each value of S_a for each ground motion, as well as S_a intensity at collapse for each ground motion. The results of the simulations were processed and analyzed to fit lognormal probability distribution functions for PSDRs, RSDRs and PFAs for each value of S_a (when collapse has not occurred yet), and to estimate the collapse capacity for each SMRF. As an example, Fig.4 shows the estimated medians for PSDR (χ_{PSDR}) as a function of $\lambda(S_a(T_1,5\%))$ for each SMRF at the 1st story, and Fig.5 shows the collapse fragility curve for each SMRF versus $\lambda(S_a(T_1,5\%))$, demonstrating that for the DBE the probability of collapse of most SMRF designs is very small (0.9% for the testbed building).
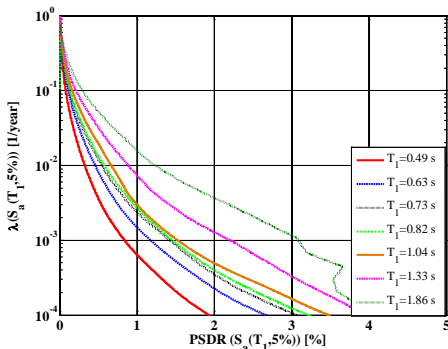

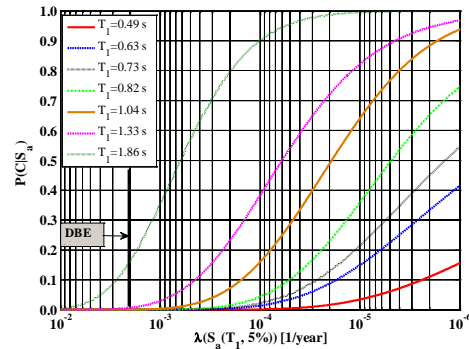Fig. 4 –χ_{PSDR} for SMRF designs at first story

Fig. 5 – Collapse fragility curves for SMRF designs

3.4 Loss estimation results

The full PEER-PBEE loss estimation methodology was implemented for each SMRF design using an inventory of structural and non-structural components corresponding to office building occupancy, with fragility functions and repair costs developed in previous studies [12, 22, 25]. The $E[L|S_a]$ versus $\lambda(S_a(T_1,5\%))$ curves for each SMRF design are shown in Fig.6, and it can be seen that for the service level earthquake (SLE), with a mean annual frequency of exceedance of 0.0139 [1/year], losses range from \$352,640 (5% of the CC of the testbed building) to \$1,688,170 (23% of the CC of the testbed building). In particular, the testbed building (T_1=1.33 s) has a loss of 13.1% (of the CC of the testbed building) for the SLE, highlighting that code-conforming designs are aimed at protecting human life but not intended to minimize losses. The EALs of each SMRF are in Fig.7 as well as the partial contributions to the EALs from the demolition (EAL_{Dem}), collapse (EAL_{Col}), and repair cases. The repair case was divided into partial contributions to the EAL from non-structural acceleration-sensitive components (EAL_{NSAS}), structural drift-sensitive components (EAL_{SDS}), non-structural drift-sensitive components (EAL_{NSDS}), and EAL_{DS} (the summation of EAL_{SDS} and EAL_{NSDS}). Fig.7 shows that as the structure becomes stiffer the reduction in EAL decreases since the EAL_{NSAS} increases rapidly while the EAL_{DS} decreases

5

marginally. This is important since the EAL might increase for very stiff structures. Fig.7 also shows that for T_1 values from 0.7 s to 1.4 s the EAL is dominated by the EAL_{DS} and that the EAL of the testbed building is 0.95%, demonstrating the significant EALs of code-conforming designs.
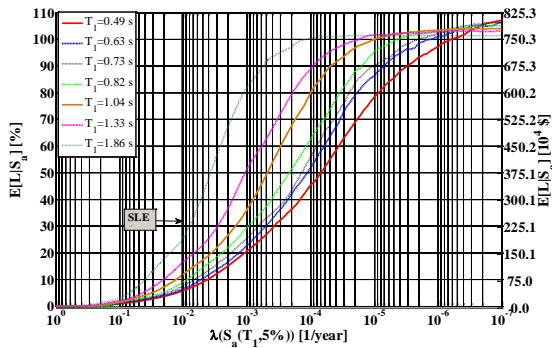

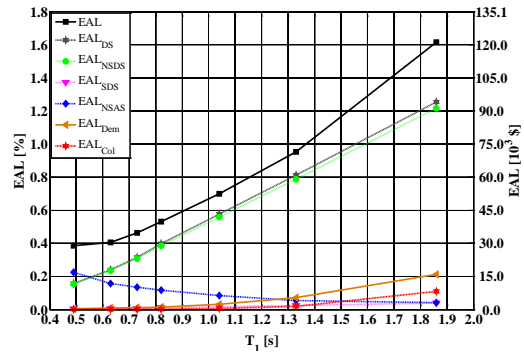Fig. 6 – $E[L|S_a]$ versus $\lambda(S_a(T_1,5\%))$ for SMRF designs

Fig. 7 – EAL for SMRF designs

3.5 Expected life cycle cost of SMRF designs

Fig.8 shows the CC, NPV(EAL), and ELCC for each SMRF design, considering a 3.9% RDR and a 50-year service life. This figure shows that the ELCCs range from 113.9% ($8,543,935) to 133.8% ($10,035,151) of the testbed CC, and the value for the testbed design was 120.8% ($9,066,127). It is important to notice that although the maximum ELCC was associated with the most flexible SMRF (T_1=1.86 s), the minimum ELCC was not associated with the stiffest SMRF. The minimum ELCC corresponds to T_1=0.73 s and would be the optimum design for a risk neutral decision maker. These findings show two things. First, the trade-off between stiffer buildings and higher construction costs becomes more expensive for very stiff structures. Second, it can be inferred that modern building codes do not provide an optimal design solution in terms of minimizing the ELCC.
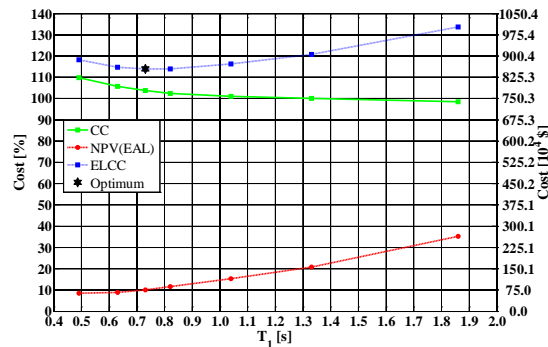

Fig. 8 – CC, NPV(EAL), and ELCC for SMRF designs

4. ELCC Assessment: Simplified Methodology

This simplified methodology was developed based on the results presented in the previous section and is recommended for low-rise steel SMRF buildings. Therefore, its application to other materials/structural systems should be further evaluated. This methodology expands Eq. (1) making it T_1 dependent, as shown in Eq.(5), allowing estimation of the T_1 value that minimizes the ELCC.

$$ELCC(T_1) = CC(T_1) + NPV(EAL(T_1)) \tag{5}$$

This simplified methodology is focused on how the stiffness, expressed as T_1, is associated with the variation of the CC and NPV(EAL) because: 1) there are previous formulations that associate T_1 with the CC; 2) steel SMRF buildings are flexible structures and, consequently, their losses are dominated by small S_a intensities

where the structures behave linearly or under the equal displacement rule. Therefore, for the EALs the stiffness of the structures is significantly more important than the strength; 3) low-rise steel SMRF buildings are first-mode dominated structures; and 4) seismic hazard curves are expressed conditioned on T_1.

4.1 Construction cost as a function of T_1

The CC of a building is a function of several variables (e.g., location, area, number of stories, materials, structural system, finishes, and occupancy). However, when only the seismic performance of a building is under study and the rest of the design variables are fixed, fewer variables have to be analyzed to account for the trade-off between improved performance and higher construction costs. Some strategies to improve the seismic performance might be the improvement of the lateral resisting system (e.g., stiffer frames or seismic protection systems) and/or the improvement of the performance of non-structural components and contents. In any case, the increment in the CC is often relatively small since most of the CC is not affected by the improvement of the seismic performance. This section focuses on the variation of the CC when the T_1 value of a SMRF of a steel low-rise building is improved over the minimum code requirements. This challenge was addressed before by Reyes [13], who proposed Eq. (6).

$$CC(T_1) = CC_{GL} + m_k(T_{GL} - T_1)^{\beta_k} \tag{6}$$

where $CC(T_1)$ and T_1 have been defined, T_{GL} is fundamental period of vibration if the building were designed only for gravity loads, CC_{GL} is the initial construction cost of the building designed only for gravity loads, and m_k and β_k are empirically-derived parameters. This study extends Eq. (6), proposing Eq. (7) for low-rise steel SMRFs.

$$CC(T_1) = CC_0 + CC_{SMRF-CCB}\left(\frac{T_{1-CCB}}{T_1}\right)^{1.33} + CC_{F-SMRF-CCB}\left(\frac{T_{1-CCB}}{T_1}\right)^{1.33 \times \frac{2}{3}} \tag{7}$$

where CC_0 is the fixed CC of the building without considering its SMRFs and the corresponding foundations of the SMRFs, $CC_{SMRF-CCB}$ is the CC of the SMRFs of a code-conforming design that meets only the minimum seismic requirements, $CC_{F-SMRF-CCB}$ is the CC of the foundation corresponding to the SMRFs of a code-conforming design, and T_{1-CCB} is the fundamental period of vibration of a code-conforming design. This formulation was developed based on: 1) the shape of the relationship between steel weight of SMRFs and their corresponding stiffness investigated for a set of 328 cruciform assemblies with strong-column weak-girder ratios between 1.0 and 1.8; 2) the direct relationship assumed between the steel weight of these SMRFs and their CC; and 3) the variation of the foundation area needed to take the additional moment from a SMRF with larger capacity, assuming a square foundation. For further information see Araya-Letelier [22]. The implementation of Eq. (7) using the testbed building as the required code-conforming design is shown in Fig.9. As seen in this figure, the proposed model provides reasonably accurate results for the variation of CC as a function of T_1.
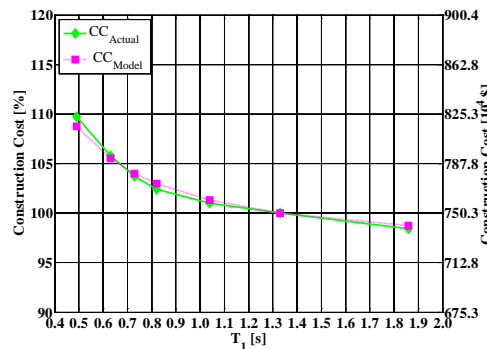

Fig. 9 – CC for SMRF designs from actual data and proposed model

4.2 Expected annual loss as a function of T_1

Reversing the terms of Eq. (3), Jalayer [26] presented the alternative calculation of the EAL shown in Eq. (8).

$$EAL = \int_{S_a=0}^{\infty} \left| \frac{dE[L|S_a]}{dS_a} \right| \lambda(S_a) dS_a \qquad (8)$$

Eq. (8) is used in this study since enables the implementation of a closed-form solution for the integral when the $E[L|S_a]$ curve is represented with a lognormal formulation and the $\lambda(S_a)$ curve is represented with a 2nd-order polynomial function (in the log-log domain) as shown later. Additionally, this study develops T_1-dependent formulations for the $E[L|S_a]$ curves and the $\lambda(S_a)$ curves as described later.

4.2.1 Expected loss conditioned on S_a as a function of T_1

The $E[L|S_a]$ curve is approximated from the $E[L_{DS}|PSDR]$ curve (expected loss of drift-sensitive (DS) components conditioned on PSDR) for a specific building (whose T_1 is the only unknown variable) without the need of IDAs. These PSDRs can be associated with S_a intensities as a function of T_1 using Eq. (9), proposed by Miranda [20], where all the terms have been defined previously. The use of Eq. (9) to estimate a uniform value of PSDR along the height for each value of T_1 is a reasonable simplification for first-mode-dominated structures.

$$PSDR \approx \beta_1 \beta_2 \frac{T_1^2 S_a}{4\pi^2 H_{roof}} \qquad (9)$$

It is important to highlight that, although the losses from drift-sensitive components represent the majority of the EAL, the approximation of the $E[L|S_a]$ from the $E[L_{DS}|PSDR]$ curve does not consider the contribution from collapse, demolition and losses from non-structural acceleration-sensitive components (NSAS). This limitation is discussed later in this study.

The calculation of the $E[L_{DS}|PSDR]$ curves requires large databases, but it is numerically easy to implement. Additionally, Ramirez and Miranda [4] have provided the $E[L_{DS}|PSDR]$ curves for several buildings. Eq. (10) shows the proposed three-parameter lognormal representation of the $E[L_{DS}|PSDR]$ curves.

$$E[L_{DS}|PSDR] = \rho_{PSDR} \Phi \left(\frac{Ln(PSDR) - Ln(\chi_{PSDR})}{\sigma_{Ln(PSDR)}} \right) \qquad (10)$$

where ρ_{PSDR} is a scale factor that multiplies the lognormal representation, Φ is the normal cumulative distribution function, χ_{PSDR} was defined previously, and $\sigma_{Ln(PSDR)}$ is the standard deviation of the natural logarithm of the PSDR. Eq. (10) is fitted to the actual data of $E[L_{DS}|PSDR]$ from the SMRF designs and provides a good representation as shown in Fig.10.
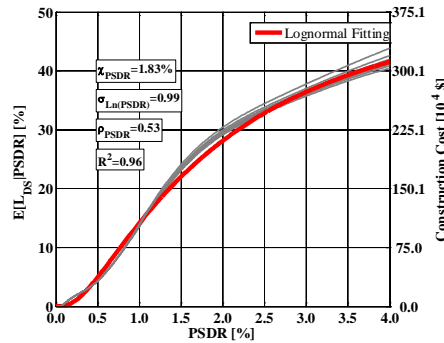

Fig. 10 – Lognormal representation and actual $E[L_{DS}|PSDR]$ curve

Substituting Eq. (9) into Eq. (10), the $E[L|S_a]$ curve (considering only DS components) can be estimated as shown in Eq. (11), whose application to actual data from the SMRF designs is shown in Fig.11, demonstrating an adequate representation, especially for the small S_a intensities that dominate the EAL calculation.

$$E[L_{DS}|S_a, T_1] = \rho_{PSDR} \Phi \left(\frac{Ln\left(\beta_1 \beta_2 \frac{T_1^2 S_a}{4\pi^2 H_{roof}}\right) - Ln(\chi_{PSDR})}{\sigma_{Ln(PSDR)}} \right) \tag{11}$$
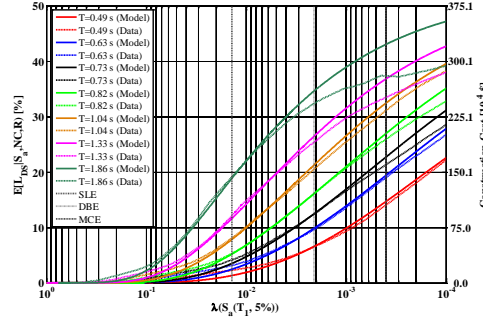

Fig. 11 – $\lambda(S_a(T_1,5\%))$ versus $E[L_{DS}|S_a,T_1]$ from actual data and from Eq. (11)

Taking the partial derivate of Eq. (11) with respect S_a, Eq. (12) is obtained, where all the terms have been defined previously. Eq. (12) will be used to calculate the EAL values using Eq. (8) later in this study.

$$\frac{\partial E[L_{DS}|S_a, T_1]}{\partial S_a} = \rho_{PSDR} \frac{1}{\beta_1 \beta_2 \frac{T_1^2 S_a}{4\pi^2 H_{roof}}^2 \sqrt{2\pi \sigma_{Ln(PSDR)}^2}} exp \left(\frac{\left(Ln\left(\beta_1 \beta_2 \frac{T_1^2 S_a}{4\pi^2 H_{roof}}\right) - Ln(\chi_{PSDR})\right)^2}{2\sigma_{Ln(PSDR)}^2} \right) \tag{12}$$

4.2.2 Seismic hazard as a function of T_1

The representation of the seismic hazard curves in the full methodology was implemented using continuous 7th-order polynomials in the log-log domain. Although these representations can be very accurate, they do not allow the implementation of a closed-form solution for solving Eq. (8). A simpler method to represent the seismic hazard curve was proposed by previous researchers [14-16], which is based on a linear representation in the log-log domain shown in Eq. (13).

$$\lambda(S_a) = k_0(S_a)^{-k} \tag{13}$$

where k_0 and k are empirical constants obtained from adjusting the linear model to S_a with λ of 0.0021 [1/year] (DBE) and 0.0004 [1/year] (MCE). Eq. (13) allows the use of a closed-form solution, but it overestimates the hazard for a large range of S_a values as shown in Fig.12(a). This figure also shows the actual data from the USGS [20], a 7th-order polynomial representation and a 2nd-order polynomial representation that allows the use of a closed-form solution for Eq. (8), which is proposed by this study in Eq. (14), where the a_i values are empirical constants derived for a given site. Fig.12(b) shows the implementation of the proposed seismic hazard representation for three T_1 values.
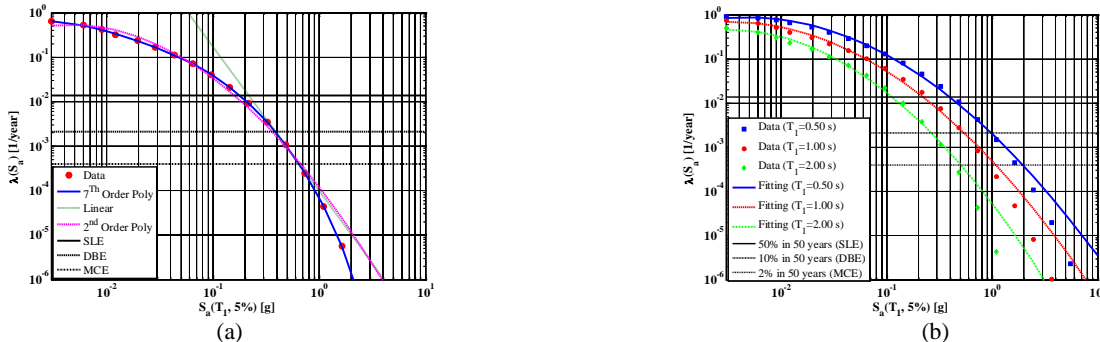

(a)   (b)

Fig. 12 – $\lambda(S_a)$ curves for selected site (33.996, -118.162): a) T_1=1.33 s; b) T_1=[0.5 s; 1.0 s; 2.0 s]

$$\lambda(S_a) = exp\left(\sum_{i=0}^{2} a_i Ln(S_a)^i\right) \tag{14}$$

To make the representation of the seismic hazard curves T_1 dependent, this study assumes that the curvature (a_2 and a_1 parameters in Eq. (14)) of each 2nd-order polynomial is fixed for a selected site but the position (a_0 parameter in Eq. (14)) is a function of T_1, as shown in Eq. (15).

$$\lambda(S_a, T_1) = exp\left(a_2 Ln(S_a)^2 + a_1 Ln(S_a) - \delta T_1^{\eta}\right) \tag{15}$$

where δ and η are empirical constants obtained performing a power fitting to the actual pairs of a_0-T_1 values. For further information see Araya-Letelier [22]. Fig.13 shows the implementation of Eq. (15).
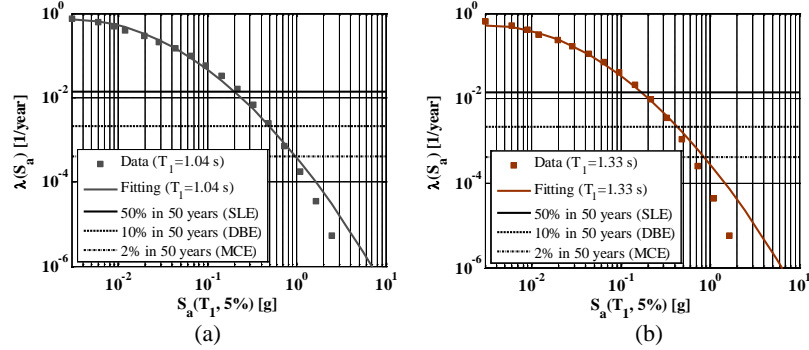

Fig. 13 – $\lambda(S_a)$ curve representations for selected site (33.996, -118.162): a) T_1=1.04 s; b) T_1=1.33 s

Substituting Eq. (12) and Eq. (15) into Eq. (8), a closed-form solution for calculating the EAL is obtained and shown in Eq. (16), where each term has been previously defined.

$$EAL(T_1) = \rho_{PSDR}^2 \sqrt{\frac{1}{\left(1 - 2a_2\sigma_{Ln(PSDR)}^2\right)}} exp\left(\frac{2(-\delta T_1^{\eta}) + 2a_2\left(Ln\left(\frac{4\pi^2 H_{roof}X_{PSDR}}{T_1^2\beta_1\beta_2}\right)\right)^2 - 4(-\delta T_1^{\eta})a_2\sigma_{Ln(PSDR)}^2 + 2a_1 Ln\left(\frac{4\pi^2 H_{roof}X_{PSDR}}{T_1^2\beta_1\beta_2}\right) + \left(a_1\sigma_{Ln(PSDR)}\right)^2}{2 - 4a_2\sigma_{Ln(PSDR)}^2}\right) \tag{16}$$

Fig.14 compares the EAL_{DS} values obtained from the simplified methodology to actual values (from the full methodology), showing that predictions are reasonably accurate for values of T_1 from 0.7 s to 1.5 s, where most of the alternative designs will be for low-rise steel SMRF buildings. Notice that Eq. (16) only calculates the EAL_{DS}. Although EAL_{DS} represents the majority of the EAL, the other components, especially EAL_{NSAS}, still need to be incorporated in the methodology. Fig.15 compares CC, NPV(EAL) and ELCC values obtained from the simplified methodology to actual values, showing again very good predictions for values of T_1 from 0.7 s to 1.5 s.
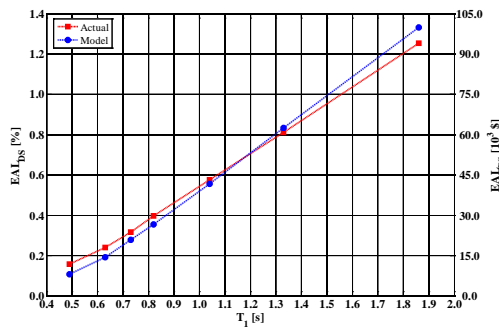

Fig. 14 – EAL_{DS} of SMRF designs (full and simplified methodology)
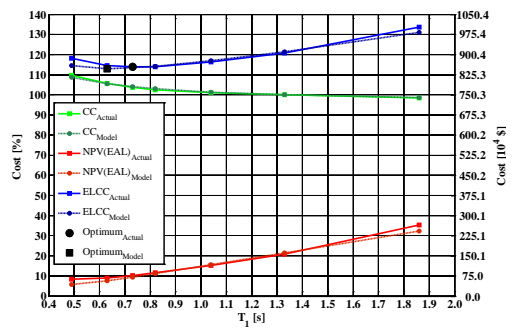
Fig. 15 – CC, NPV(EAL) and ELCC values of SMRF designs (full and simplified methodology)

10

5. Conclusions

This study develops a simplified methodology to estimate the ELCC of low-rise steel SMRF buildings as a function of the stiffness (T_1). These structures are flexible and first-mode dominated, and their EALs are dominated by small S_a values where the structures behave linearly or under the equal displacement rule with a relatively uniform PSDR distribution along the height. This simplified methodology is based on actual results of EALs and CCs from seven 4-story steel SMRF buildings designed with varying degrees of lateral stiffness, including a testbed building that only meets the minimum code requirements. These numeric results show significant losses for the testbed building, implying that modern building codes do not provide an optimal design in terms of minimizing the ELCC.

The proposed simplified methodology provides two equations to estimate the $CC(T_1)$ and $EAL(T_1)$, both required components of $ELCC(T_1)$. To estimate the $CC(T_1)$ a previous formulation was extended incorporating the additional cost of SMRFs and their corresponding foundations, and it provides good prediction results when compared to the actual results developed from construction cost databases. The $EAL(T_1)$ formulation requires the estimation of $E[L|S_a,T_1]$ and $\lambda(S_a,T_1)$. This study proposes a lognormal representation of the $E[L|S_a,T_1]$ curve obtained using the $E[L_{DS}|PSDR]$ curve and a simple formulation that relates the PSDRs to the S_a intensities as a function of T_1, eliminating the need for IDAs. Regarding $\lambda(S_a,T_1)$, this study proposes a 2nd-order polynomial representation (in log-log domain) that is T_1 dependent and represents the hazard significantly better than a linear representation previously proposed. The proposed formulations for $E[L|S_a,T_1]$ and $\lambda(S_a,T_1)$ lead to a closed-form solution for the calculation of the $EAL(T_1)$, eliminating the need for numerical integrations.

Values obtained from the simplified methodology are compared to actual values, and predictions are shown to be very good for values of T_1 from 0.7 s to 1.5 s, where most of the alternative designs will be for low-rise steel SMRF buildings.

6. Acknowledgements

7. References

[1] EERI (2010): The M_w 8.8 Chile earthquake of February 27, 2010. *EERI Special Earthquake Report*, Earthquake Engineering Research Institute (EERI), Oakland,CA.

[2] EERI (2011): The M 6.3 Christchurch, New Zealand earthquake of February 22, 2011. *EERI Special Earthquake Report*, Earthquake Engineering Research Institute (EERI), Oakland, CA.

[3] Krawinkler H, Miranda E (2004): Performance-based earthquake engineering. In Y. Borzognia and V. Bertero (Ed.), *Earthquake Engineering: From Engineering Seismology to Performance-Based Engineering, 1st edition* (pp 9-1 to 9-59). CRC Press.

[4] Ramirez CM, Miranda E (2009): Building-specific loss estimation methods and tools for simplified performance-based earthquake engineering. *Report No. 171*. The John A. Blume Earthquake Engineering Center, Stanford University, Stanford, CA.

[5] Vanmarcke EH, Cornell CA, Whitman RV, Reed JW (1973): Methodology for optimum seismic design. *5th World Conference on Earthquake Engineering*, Rome, Italy. Vol. 2, 2521-2530.

[6] Polak E, Pister KS, Ray D (1976): Optimal design of framed structures subjected to earthquakes. *Engineering Optimization,* **2** (1), 65-71.

[7] Rosenblueth E, Asfura A (1976): Optimum seismic design of linear shear buildings. *Journal of the Structural Division*, **102** (5), 1077–1084.

[8] Zagajeski SW, Bertero VV (1977): Computer-aided optimum seismic design of ductile reinforced concrete moment-resisting frames. Earthquake Engineering Research Center, College of Engineering, University of California, Berkeley, CA.

[9] Esteva L, Díaz-López J, García-Pérez J, Sierra G, Ismael E (2002): Life-cycle optimization in the establishment of performance-acceptance parameters for sesimic design. *Structural Safety,* **24** (2), 187-204.

[10] Liu M, Burns SA, Wen YK (2003): Optimal seismic design of steel frame buildings based on life cycle cost considerations. *Earthquake Engineering and Structural Dynamics,* **32** (9), 1313-1332.

[11] Goda K, Hong HP (2006): Optimal seismic design considering risk attitude, societal tolerable risk, and life quality criterion. *Journal of Structural Engineering,* **132** (12), 2027-2035.

[12] ATC (2012): Seismic performance assessment of buildings. FEMA P-58, Federal Emergency Management Agency (FEMA), Washington, DC.

[13] Reyes C (1999): The serviceability limit state in the earthquake resistant design of buildings. Doctoral Thesis (in Spanish), School of Engineering, National University of Mexico, Mexico City, Mexico.

[14] Sewelll RT, Toro GR, McGuire RK (1991): Impact of ground motion characterization on conservatism and variability in seismic risk estimated. *Risk engineering report to USNRC.*

[15] Kennedy RC, Short SA (1994): Basis for seismic provisions of DOE-STD-1020. *Report No. UCRL-CR-111478, S/C-B235302*, Brookhaven National Lab. BNL-52418. Lawrence Livermore National Lab.

[16] Luco N, Cornell CA (1998): Effects of random connection fractures on demands and reliability for a 3-story pre-Northridge SMRF structure. *Proc., 6th U.S. National Conference on Earthquake Engineering*, Seattle, Washington.

[17] Dell'Isola AJ, Kirk SJ (2003): *Life cycle costing for facilities: economic analysis for owners and professionals in planning, programming, and real estate development: designing, specifying, and construction: maintenance, operations, and procurement*, Reed Construction Data, Kingston, MA.

[18] Balboni B (Ed.) (2010): *2010 RS Means Square Foot Costs.* R.S. Means Company. Kingston, MA.

[19] Lignos DG, Krawinkler H (2012): Sidesway collapse of deteriorating structural systems under seismic excitations. *Report No. 177.* The John A. Blume Earthquake Engineering Center, Stanford University, Stanford, CA.

[20] Miranda E (1999): Approximate seismic lateral deformation demands in multistory buildings. *Journal of Structural Engineering*, **125** (4), 417-425.

[21] USGS (2011). Java Ground Motion Parameter Calculator, Version 5.1.0. United States Geological Survey (USGS).

[22] Araya-Letelier G (2014): Design of Building Structural Systems and Enhanced Partition Walls to Improve Life Cycle Costs Associated with Risk of Earthquake Damage. *Doctoral dissertation*, Stanford University, Stanford CA.

[23] Goulet CA, Haselton CB, Mitrani-Reiser J, Beck JL, Deierlein GG, Porter KA, Stewart JP (2007): Evaluation of the seismic performance of a code-conforming reinforced-concrete frame building - from seismic hazard to collapse safety and economic losses. *Earthquake Engineering and Structural Dynamics*, **36** (13), 1973 - 1997.

[24] Haselton CB, Mitrani-Reiser J, Goulet C, Deierlein GG, Beck J, Porter KA, Stewart J, Taciroglu E (2008): An assessment to benchmark the seismic performance of a code-conforming reinforced-concrete moment-frame building. *PEER Report 2007/12*, Pacific Earthquake Engineering Research Center, Berkeley, CA.

[25] Aslani H, Miranda E (2005): Probabilistic earthquake loss estimation and loss disaggregation in buildings. *Report No. 157*. The John A. Blume Earthquake Engineering Center, Stanford University, Stanford, CA.

[26] Jalayer F (2003): Direct probabilistic seismic analysis: implementing non-linear dynamic assessments. *Doctoral dissertation*, Stanford University, Stanford CA.